Leptonic invariant mass spectrum of the $B \to X_c l \bar{\nu}_l$

Mateusz Czaja[1]

In collaboration with
Mikołaj Misiak[1], and Abdur Rehman[2]

25.09.2024

[1] Institute of Theoretical Physics, University of Warsaw
[2] Faculty of Science - Physics, University of Alberta

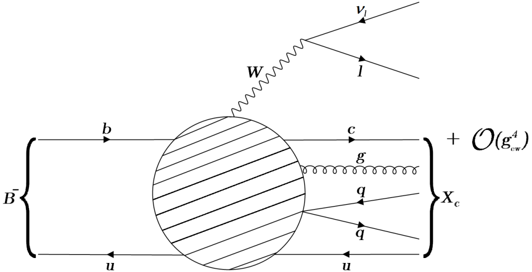

- At the leading order in EW interactions, the inclusive differential rate factorizes into hadronic and leptonic parts:

$$\frac{d\Gamma}{dq^2 dr^2 dE_l} \propto G_F^2 |V_{cb}|^2 W^{\alpha\beta} L_{\alpha\beta},$$

$q \equiv k_l + k_{\bar{\nu}}$, and $r \equiv p_B - q$.

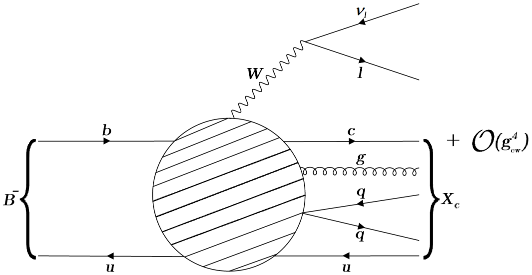

- At the leading order in EW interactions, the inclusive differential rate factorizes into hadronic and leptonic parts:

$$\frac{d\Gamma}{dq^2 dr^2 dE_l} \propto G_F^2 |V_{cb}|^2 W^{\alpha\beta} L_{\alpha\beta},$$

$q \equiv k_l + k_{\bar{\nu}}$, and $r \equiv p_B - q$.

- The leptonic tensor is fixed to all orders in QCD:

$$L^{\alpha\beta} \equiv \frac{1}{2} \sum_{s_l s_{\bar{\nu}}} A_l^{\alpha} A_l^{\dagger\beta}, \qquad A_l^{\alpha} \equiv \bar{u}_l^{(s_l)} \gamma^{\alpha} P_L v_{\bar{\nu}}^{(s_{\bar{\nu}})}.$$

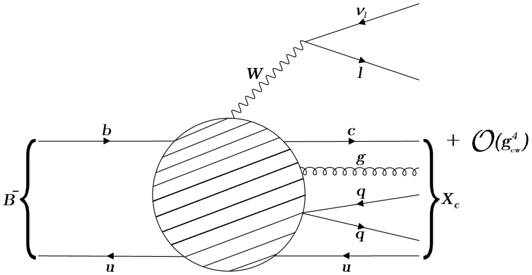

- At the leading order in EW interactions, the inclusive differential rate factorizes into hadronic and leptonic parts:

$$\frac{d\Gamma}{dq^2 dr^2 dE_l} \propto G_F^2 |V_{cb}|^2 W^{\alpha\beta} L_{\alpha\beta},$$

$q \equiv k_l + k_{\bar{\nu}}$, and $r \equiv p_B - q$.

- The leptonic tensor is fixed to all orders in QCD:

$$L^{\alpha\beta} \equiv \frac{1}{2} \sum_{s_l s_{\bar{\nu}}} A_l^\alpha A_l^{\dagger\beta}, \qquad A_l^\alpha \equiv \bar{u}_l^{(s_l)} \gamma^\alpha P_L v_{\bar{\nu}}^{(s_{\bar{\nu}})}.$$

- The hadronic tensor $W^{\alpha\beta}$ is defined as

$$W^{\alpha\beta} \equiv \sum_{X_c} \langle B | J_H^\alpha | X_c \rangle \langle X_c | J_H^{\dagger\beta} | B \rangle, \qquad J_H^\alpha \equiv \bar{b} \gamma^\alpha P_L c,$$

- The optical theorem and the Operator Product Expansion can be used to write $W^{\alpha\beta}$ as a series of matrix elements suppressed by powers of Λ_{QCD}/m_b:

$$W^{\alpha\beta} \propto \mathrm{Im} \sum_{k\geq 0} \frac{C_k \langle B|O_k^{(n)\alpha\beta}|B\rangle}{m_b^{n(k)}}, \text{ where } \frac{\langle B|O_k^{(n)\alpha\beta}|B\rangle}{\langle B|B\rangle} \sim \Lambda_{QCD}^n.$$

- The optical theorem and the Operator Product Expansion can be used to write $W^{\alpha\beta}$ as a series of matrix elements suppressed by powers of Λ_{QCD}/m_b:

$$W^{\alpha\beta} \propto \mathrm{Im} \sum_{k\geq 0} \frac{C_k \langle B|O_k^{(n)\alpha\beta}|B\rangle}{m_b^{n(k)}}, \text{ where } \frac{\langle B|O_k^{(n)\alpha\beta}|B\rangle}{\langle B|B\rangle} \sim \Lambda_{QCD}^n.$$

- The Wilson coefficients C_k are computed perturbatively in powers of α_s in a matching between partonic QCD and HQE.

- The optical theorem and the Operator Product Expansion can be used to write $W^{\alpha\beta}$ as a series of matrix elements suppressed by powers of Λ_{QCD}/m_b:

$$W^{\alpha\beta} \propto \text{Im} \sum_{k\geq 0} \frac{C_k \langle B|O_k^{(n)\alpha\beta}|B\rangle}{m_b^{n(k)}}, \text{ where } \frac{\langle B|O_k^{(n)\alpha\beta}|B\rangle}{\langle B|B\rangle} \sim \Lambda_{QCD}^n.$$

- The Wilson coefficients C_k are computed perturbatively in powers of α_s in a matching between partonic QCD and HQE.
- At the LO and NLO:

$$\langle B|O_k^{(0)}|B\rangle = 2m_B \left(1 + \mathcal{O}\left(\frac{\Lambda_{QCD}^2}{m_b^2}\right)\right), \; O_k^{(1)} = 0|_{EOM} + \mathcal{O}\left(\frac{\Lambda_{QCD}^2}{m_b^2}\right)$$

- The optical theorem and the Operator Product Expansion can be used to write $W^{\alpha\beta}$ as a series of matrix elements suppressed by powers of Λ_{QCD}/m_b:

$$W^{\alpha\beta} \propto \text{Im} \sum_{k\geq 0} \frac{C_k \langle B|O_k^{(n)\alpha\beta}|B\rangle}{m_b^{n(k)}}, \text{ where } \frac{\langle B|O_k^{(n)\alpha\beta}|B\rangle}{\langle B|B\rangle} \sim \Lambda_{QCD}^n.$$

- The Wilson coefficients C_k are computed perturbatively in powers of α_s in a matching between partonic QCD and HQE.
- At the LO and NLO:

$$\langle B|O_k^{(0)}|B\rangle = 2m_B \left(1 + \mathcal{O}\left(\frac{\Lambda_{QCD}^2}{m_b^2}\right)\right), \; O_k^{(1)} = 0|_{EOM} + \mathcal{O}\left(\frac{\Lambda_{QCD}^2}{m_b^2}\right)$$

- The same procedure can be performed for any spectral moment:

$$M[w] \propto G_F^2 |V_{cb}|^2 \int [dPS] w[v, k_l, k_\nu] W^{\alpha\beta} L_{\alpha\beta} = G_F^2 |V_{cb}|^2 \text{Im} \sum_{k\geq 0} \frac{\hat{C}_k[w] \langle B|O_k^{(n)}|B\rangle}{m_b^{n(k)}}.$$

- The optical theorem and the Operator Product Expansion can be used to write $W^{\alpha\beta}$ as a series of matrix elements suppressed by powers of Λ_{QCD}/m_b:

$$W^{\alpha\beta} \propto \mathrm{Im} \sum_{k\geq 0} \frac{C_k \langle B|O_k^{(n)\alpha\beta}|B\rangle}{m_b^{n(k)}}, \text{ where } \frac{\langle B|O_k^{(n)\alpha\beta}|B\rangle}{\langle B|B\rangle} \sim \Lambda_{QCD}^n.$$

- The Wilson coefficients C_k are computed perturbatively in powers of α_s in a matching between partonic QCD and HQE.
- At the LO and NLO:

$$\langle B|O_k^{(0)}|B\rangle = 2m_B\left(1 + \mathcal{O}\left(\frac{\Lambda_{QCD}^2}{m_b^2}\right)\right), \; O_k^{(1)} = 0|_{EOM} + \mathcal{O}\left(\frac{\Lambda_{QCD}^2}{m_b^2}\right)$$

- The same procedure can be performed for any spectral moment:

$$M[w] \propto G_F^2|V_{cb}|^2 \int [dPS] w[v, k_l, k_\nu] W^{\alpha\beta} L_{\alpha\beta} = G_F^2|V_{cb}|^2 \mathrm{Im} \sum_{k\geq 0} \frac{\hat{C}_k[w] \langle B|O_k^{(n)}|B\rangle}{m_b^{n(k)}}.$$

- Moments with weight functions w independent of the B meson velocity v are called reparametrization invariant (RPI). The Wilson coefficients of such moments satisfy linear relations that allow one to eliminate some of them from the OPE [T. Mannel, K. K. Vos, JHEP 06 (2018) 115].

- The optical theorem and the Operator Product Expansion can be used to write $W^{\alpha\beta}$ as a series of matrix elements suppressed by powers of Λ_{QCD}/m_b:

$$W^{\alpha\beta} \propto \mathrm{Im} \sum_{k\geq 0} \frac{C_k \langle B|O_k^{(n)\alpha\beta}|B\rangle}{m_b^{n(k)}}, \text{ where } \frac{\langle B|O_k^{(n)\alpha\beta}|B\rangle}{\langle B|B\rangle} \sim \Lambda_{QCD}^n.$$

- The Wilson coefficients C_k are computed perturbatively in powers of α_s in a matching between partonic QCD and HQE.
- At the LO and NLO:

$$\langle B|O_k^{(0)}|B\rangle = 2m_B \left(1 + \mathcal{O}\left(\frac{\Lambda_{QCD}^2}{m_b^2}\right)\right), \; O_k^{(1)} = 0|_{EOM} + \mathcal{O}\left(\frac{\Lambda_{QCD}^2}{m_b^2}\right)$$

- The same procedure can be performed for any spectral moment:

$$M[w] \propto G_F^2|V_{cb}|^2 \int [dPS] w[v, k_l, k_\nu] W^{\alpha\beta} L_{\alpha\beta} = G_F^2|V_{cb}|^2 \mathrm{Im} \sum_{k\geq 0} \frac{\hat{C}_k[w] \langle B|O_k^{(n)}|B\rangle}{m_b^{n(k)}}.$$

- Moments with weight functions w independent of the B meson velocity v are called reparametrization invariant (RPI). The Wilson coefficients of such moments satisfy linear relations that allow one to eliminate some of them from the OPE [T. Mannel, K. K. Vos, JHEP 06 (2018) 115].
- Example: the q^2 spectrum $\left(w = \delta[(k_l + k_\nu)^2 - q^2]\right)$ and its moments $\left(w = (k_l + k_\nu)^{2k}\right)$.

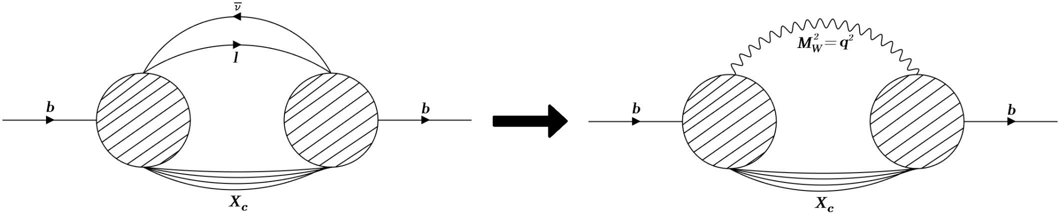

$$L^{\alpha\beta} \equiv \frac{1}{2}\sum_{s_l s_{\bar{\nu}}} A_l^{\alpha} A_l^{\dagger\beta} = k_l^{\alpha} k_{\bar{\nu}}^{\beta} + k_l^{\beta} k_{\bar{\nu}}^{\alpha} - (k_l k_{\bar{\nu}}) g^{\alpha\beta} - i\epsilon^{\alpha\rho\beta\sigma} k_{l_\rho} k_{\bar{\nu}_\sigma}, \qquad A_l^{\alpha} \equiv \bar{u}_l^{(s_l)} \gamma^{\alpha} P_L v_{\bar{\nu}}^{(s_{\bar{\nu}})}.$$

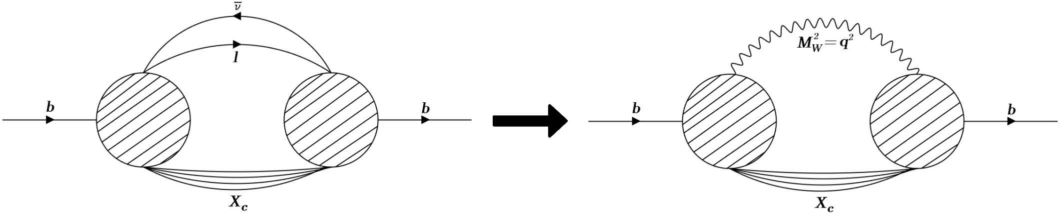

$$L^{\alpha\beta} \equiv \frac{1}{2} \sum_{s_l s_{\bar{\nu}}} A_l^{\alpha} A_l^{\dagger\beta} = k_l^{\alpha} k_{\bar{\nu}}^{\beta} + k_l^{\beta} k_{\bar{\nu}}^{\alpha} - (k_l k_{\bar{\nu}}) g^{\alpha\beta} - i\epsilon^{\alpha\rho\beta\sigma} k_{l_\rho} k_{\bar{\nu}_\sigma}, \qquad A_l^{\alpha} \equiv \bar{u}_l^{(s_l)} \gamma^{\alpha} P_L v_{\bar{\nu}}^{(s_{\bar{\nu}})}.$$

- Assuming massless leptons, one can integrate $L^{\alpha\beta}$ over E_l to obtain

$$\frac{d\Gamma}{dq^2 dr^2} \propto G_F^2 |V_{cb}|^2 W^{\alpha\beta} \int dE_l L_{\alpha\beta} \propto G_F^2 |V_{cb}|^2 \frac{|\vec{q}|}{3} (q_\alpha q_\beta - q^2 g_{\alpha\beta}) W^{\alpha\beta},$$

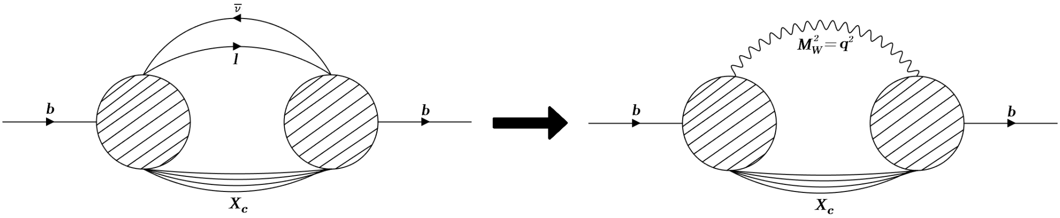

$$L^{\alpha\beta} \equiv \frac{1}{2}\sum_{s_l s_{\bar{\nu}}} A_l^\alpha A_l^{\dagger\beta} = k_l^\alpha k_{\bar{\nu}}^\beta + k_l^\beta k_{\bar{\nu}}^\alpha - (k_l k_{\bar{\nu}})g^{\alpha\beta} - i\epsilon^{\alpha\rho\beta\sigma} k_{l_\rho} k_{\bar{\nu}_\sigma}, \qquad A_l^\alpha \equiv \bar{u}_l^{(s_l)}\gamma^\alpha P_L v_{\bar{\nu}}^{(s_{\bar{\nu}})}.$$

- Assuming massless leptons, one can integrate $L^{\alpha\beta}$ over E_l to obtain

$$\frac{d\Gamma}{dq^2 dr^2} \propto G_F^2 |V_{cb}|^2 W^{\alpha\beta} \int dE_l L_{\alpha\beta} \propto G_F^2 |V_{cb}|^2 \frac{|\vec{q}|}{3}(q_\alpha q_\beta - q^2 g_{\alpha\beta})W^{\alpha\beta},$$

- The transverse structure can be reproduced by polarization vectors ε_μ of an auxiliary final state W-boson with $M_W^2 = q^2$:

$$\sum_{polarizations} \varepsilon_\alpha \varepsilon_\beta = \frac{q_\alpha q_\beta - q^2 g_{\alpha\beta}}{q^2} \propto \int dE_l L_{\alpha\beta} \Longrightarrow \frac{d\Gamma}{d\tilde{q}^2} = \frac{\tilde{q}^2}{48\pi^2}\Gamma_W, \qquad \tilde{q}^2 \equiv \frac{q^2}{M_W^2}.$$

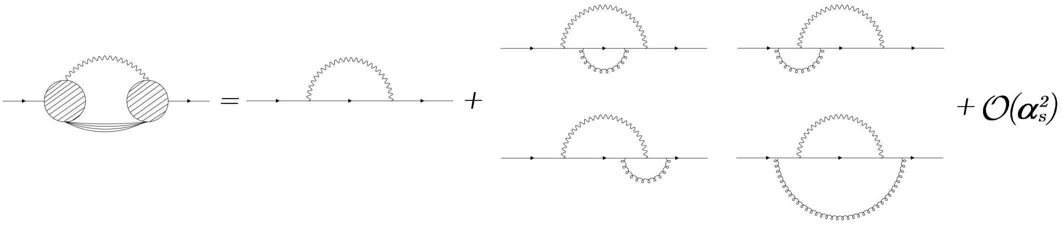

$$\frac{d\Gamma}{d\tilde{q}^2} = \frac{\tilde{q}^2}{48\pi^2}\Gamma_W$$

- The rate Γ_W is computed in perturbative QCD in powers of α_s.

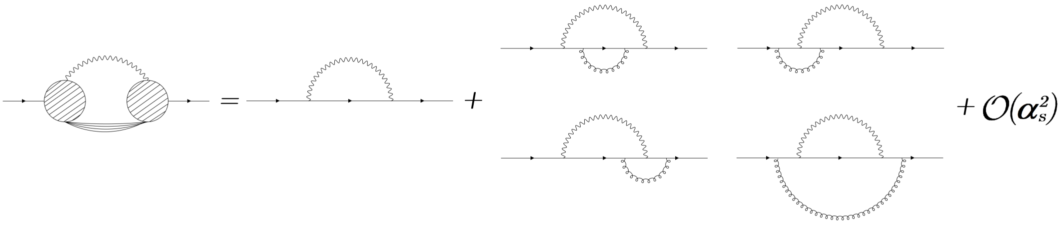

$$\frac{d\Gamma}{d\tilde{q}^2} = \frac{\tilde{q}^2}{48\pi^2}\Gamma_W$$

- The rate Γ_W is computed in perturbative QCD in powers of α_s.
- The replacement $(B \to X_c l\bar{\nu}) \longrightarrow (B \to X_c W)$ allows us to retain the q^2 dependence of the process that would normally be integrated over when using the optical theorem.

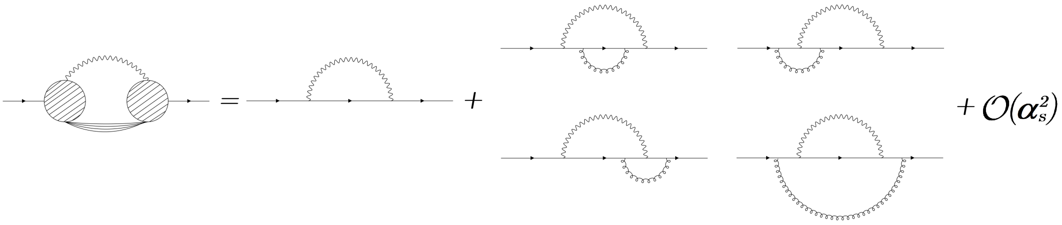

$$\frac{d\Gamma}{d\tilde{q}^2} = \frac{\tilde{q}^2}{48\pi^2}\Gamma_W$$

- The rate Γ_W is computed in perturbative QCD in powers of α_s.
- The replacement $(B \to X_c l\bar{\nu}) \longrightarrow (B \to X_c W)$ allows us to retain the q^2 dependence of the process that would normally be integrated over when using the optical theorem.
- Additionally, the lepton loop is integrated out for the price of an additional scale q^2.

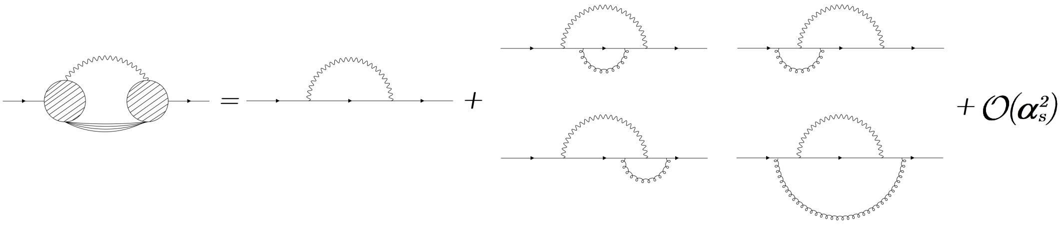

$$\frac{d\Gamma}{d\tilde{q}^2} = \frac{\tilde{q}^2}{48\pi^2}\Gamma_W$$

- The rate Γ_W is computed in perturbative QCD in powers of α_s.
- The replacement $(B \to X_c l\bar{\nu}) \longrightarrow (B \to X_c W)$ allows us to retain the q^2 dependence of the process that would normally be integrated over when using the optical theorem.
- Additionally, the lepton loop is integrated out for the price of an additional scale q^2.
- Using this method, we computed the partonic part of the q^2 spectrum, including the $\mathcal{O}(\alpha_s^2)$ correction.

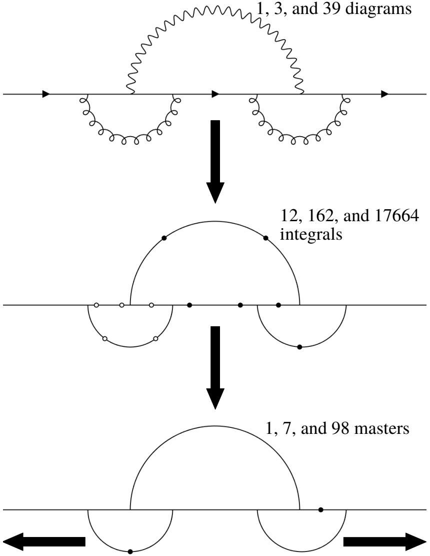
1, 3, and 39 diagrams
12, 162, and 17664
integrals
1, 7, and 98 masters

Analytic solutions:
([M. Fael and F. Herren, JHEP 05 (2024) 287])

- The DEs for a large class of integrals can be solved using the differential equations in the canonical form method.
- The boundary condition was found using `AMFlow`. [arXiv:2201.11669]
- Solution given in terms of Goncharov Polylogarithms.
- No analytic solution known for integrals with 3 cut charm quarks.

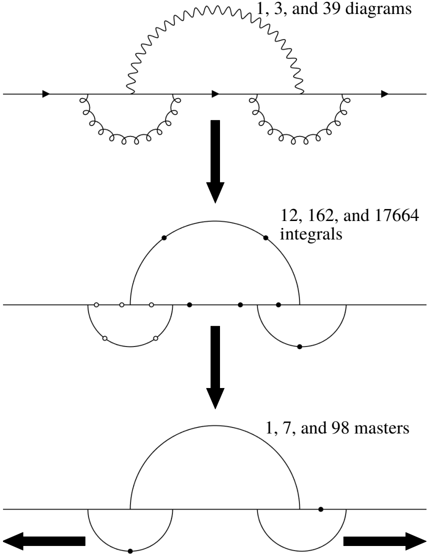

Analytic solutions:
([M. Fael and F. Herren, JHEP 05 (2024) 287])

- The DEs for a large class of integrals can be solved using the differential equations in the canonical form method.
- The boundary condition was found using `AMFlow`. [arXiv:2201.11669]
- Solution given in terms of Goncharov Polylogarithms.
- No analytic solution known for integrals with 3 cut charm quarks.

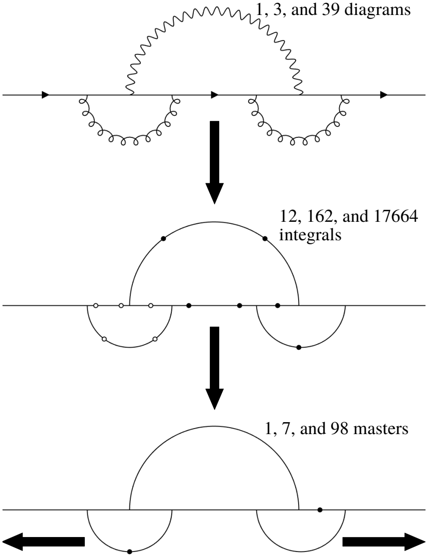

Fits to numerical solutions:
([arXiv:2410.XXXXX])

- Dense scans in the (m_c, q^2) space using `AMFlow`.
- Numerical results used for fits of elementary functions.
- Accuracy of the more than 4 significant digits when compared with exact results, far higher than experimental precision.
- The fully inlusive spectrum and the triple charm contribution can be computed.

- Scalar Feynman integrals can be solved by deriving and solving ODEs in different quantities as free variables. Usually, ratios of masses or scalar products are used.

- Scalar Feynman integrals can be solved by deriving and solving ODEs in different quantities as free variables. Usually, ratios of masses or scalar products are used.
- In the auxiliary mass flow method, the Feynman regulator η is treated as a free variable instead:

$$I_{a_1 a_2}(q^2, m_c^2) = \lim_{\eta \to 0^+} \int_{\mathbb{M}^D} \frac{d^D k}{(2\pi)^D} \frac{1}{\left(k^2 - m_c^2 + i\eta\right)^{a_1}} \frac{1}{\left((p_b - k)^2 - q^2 + i\eta\right)^{a_2}} \equiv \lim_{\eta \to 0^+} \tilde{I}_{a_1 a_2}(q^2, \eta)$$

- Scalar Feynman integrals can be solved by deriving and solving ODEs in different quantities as free variables. Usually, ratios of masses or scalar products are used.
- In the auxiliary mass flow method, the Feynman regulator η is treated as a free variable instead:

$$I_{a_1 a_2}(q^2, m_c^2) = \lim_{\eta \to 0^+} \int_{\mathbb{M}^D} \frac{d^D k}{(2\pi)^D} \frac{1}{\left(k^2 - m_c^2 + i\eta\right)^{a_1}} \frac{1}{\left((p_b - k)^2 - q^2 + i\eta\right)^{a_2}} \equiv \lim_{\eta \to 0^+} \tilde{I}_{a_1 a_2}(q^2, \eta)$$

- One can set up ODEs for $\tilde{I}_k(q^2, m_c^2, \eta)$ in η using IBP reduction:

$$\frac{d\tilde{I}_k}{d\eta} = \sum_l M_{kl}(\eta, q^2, m_c^2, \epsilon)\tilde{I}_l.$$

- Scalar Feynman integrals can be solved by deriving and solving ODEs in different quantities as free variables. Usually, ratios of masses or scalar products are used.
- In the auxiliary mass flow method, the Feynman regulator η is treated as a free variable instead:

$$I_{a_1 a_2}(q^2, m_c^2) = \lim_{\eta \to 0^+} \int_{\mathbb{M}^D} \frac{d^D k}{(2\pi)^D} \frac{1}{\left(k^2 - m_c^2 + i\eta\right)^{a_1}} \frac{1}{\left((p_b - k)^2 - q^2 + i\eta\right)^{a_2}} \equiv \lim_{\eta \to 0^+} \tilde{I}_{a_1 a_2}(q^2, \eta)$$

- One can set up ODEs for $\tilde{I}_k(q^2, m_c^2, \eta)$ in η using IBP reduction:

$$\frac{d\tilde{I}_k}{d\eta} = \sum_l M_{kl}(\eta, q^2, m_c^2, \epsilon)\tilde{I}_l.$$

- A convenient point for a boundary condition is in the $\eta \to +i\infty$ limit. For such a choice, the master integrals reduce to tadpoles with all masses equal to $\sqrt{\eta}$.

$$\tilde{I}_{a_1 a_2}(q^2, \eta) \xrightarrow[\eta \to +i\infty]{} \int_{\mathbb{M}^D} \frac{d^D k}{(2\pi)^D} \frac{1}{\left(k^2 - \eta\right)^{a_1 + a_2}} =$$

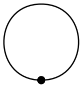

- Numerical results for such tadpoles are available up to 5 loops.

- Scalar Feynman integrals can be solved by deriving and solving ODEs in different quantities as free variables. Usually, ratios of masses or scalar products are used.
- In the auxiliary mass flow method, the Feynman regulator η is treated as a free variable instead:

$$I_{a_1 a_2}(q^2, m_c^2) = \lim_{\eta \to 0^+} \int_{\mathbb{M}^D} \frac{d^D k}{(2\pi)^D} \frac{1}{\left(k^2 - m_c^2 + i\eta\right)^{a_1}} \frac{1}{\left((p_b - k)^2 - q^2 + i\eta\right)^{a_2}} \equiv \lim_{\eta \to 0^+} \tilde{I}_{a_1 a_2}(q^2, \eta)$$

- One can set up ODEs for $\tilde{I}_k(q^2, m_c^2, \eta)$ in η using IBP reduction:

$$\frac{d\tilde{I}_k}{d\eta} = \sum_l M_{kl}(\eta, q^2, m_c^2, \epsilon) \tilde{I}_l.$$

- A convenient point for a boundary condition is in the $\eta \to +i\infty$ limit. For such a choice, the master integrals reduce to tadpoles with all masses equal to $\sqrt{\eta}$.

$$\tilde{I}_{a_1 a_2}(q^2, \eta) \xrightarrow[\eta \to +i\infty]{} \int_{\mathbb{M}^D} \frac{d^D k}{(2\pi)^D} \frac{1}{\left(k^2 - \eta\right)^{a_1 + a_2}} =$$

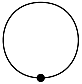

- Numerical results for such tadpoles are available up to 5 loops.
- The auxiliary mass flow method was automated in the `Mathematica` package `AMFlow` [X. Liu and Y.-Q. Ma, Comput.Phys.Commun. 283 (2023) 108565]. It allows for efficient numerical evaluation of multi-loop master integrals with arbitrary precision.

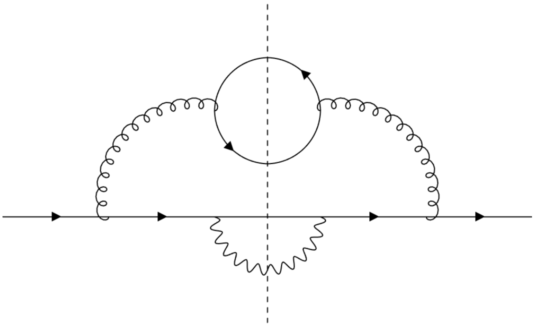

- After computing the 98 masters without cuts needed for the fully inclusive correction, we isolate the contribution from the $b \to ccc l \nu$ channel.

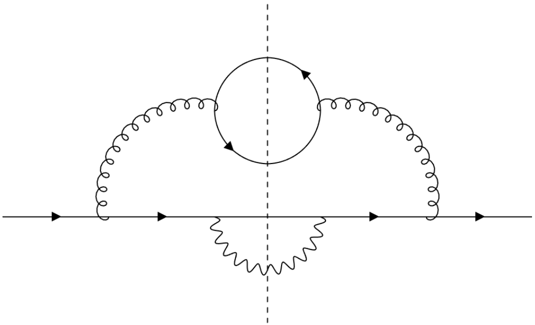

- After computing the 98 masters without cuts needed for the fully inclusive correction, we isolate the contribution from the $b \to ccc l\nu$ channel.
- Due to the small range of allowed values of q^2/m_b^2, the HQE of the triple charm spectrum is expected to be badly convergent. Fortunately, the triple charm width is strongly phase-space suppressed.

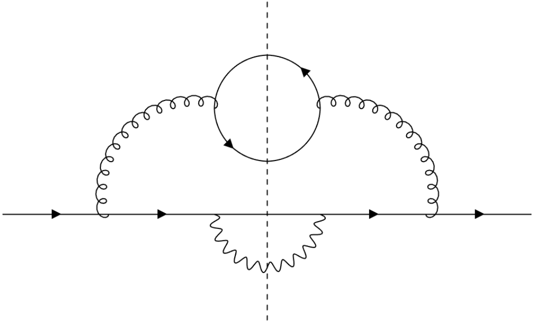

- After computing the 98 masters without cuts needed for the fully inclusive correction, we isolate the contribution from the $b \to ccc l \nu$ channel.
- Due to the small range of allowed values of q^2/m_b^2, the HQE of the triple charm spectrum is expected to be badly convergent. Fortunately, the triple charm width is strongly phase-space suppressed.
- We computed the 22 cut masters contributing to the $b \to ccc l \nu$ numerically in the same way as the fully inclusive correction. `AMFlow` allows for a simple inclusion of unitary cuts:

$$\int_{\mathbb{M}^D} \frac{d^D k}{(2\pi)^D} \delta(k^2 - m^2) J(k) = \frac{1}{2\pi i} \lim_{\eta \to 0^+} \int_{\mathbb{M}^D} \frac{d^D k}{(2\pi)^D} \left(\frac{1}{k^2 - m^2 + i\eta} - \frac{1}{k^2 - m^2 - i\eta} \right) J(k).$$

- The fully inclusive spectrum was computed numerically with the precision of 60 significant digits for 682 points in the $(q^2/m_b^2, m_c/m_b) \equiv (\bar{q}^2, \bar{m}_c)$ space, ranging from $\bar{m}_c = 0.14$ to $\bar{m}_c = 0.33$. The triple-charm correction was computed for 650 points.

- The fully inclusive spectrum was computed numerically with the precision of 60 significant digits for 682 points in the $(q^2/m_b^2, m_c/m_b) \equiv (\bar{q}^2, \bar{m}_c)$ space, ranging from $\bar{m}_c = 0.14$ to $\bar{m}_c = 0.33$. The triple-charm correction was computed for 650 points.
- The results were used to perform a fits with the following ansatz:

$$\frac{d\Gamma^{(2)}_{3c}}{dq^2} = m_b^3 G_F^2 |V_{cb}|^2 L_{3c}^{\frac{7}{2}} \sum_{jk} C^{(3c)}_{jk} \bar{m}_c^j \bar{q}^{2k}, \qquad L_{3c} \equiv \left(\bar{q}^2 - (1+3\bar{m}_c)^2\right)\left(\hat{q}^2 - (1-3\bar{m}_c)^2\right)$$

$$\frac{d\Gamma^{(2)}_{1c}}{dq^2} = m_b^3 G_F^2 |V_{cb}|^2 L_{1c} \sum_{jkl} C^{(1c)}_{jkl} \bar{m}_c^j \bar{q}^{2k} \log^l L_{1c}, \quad L_{1c} \equiv \left(\bar{q}^2 - (1+\bar{m}_c)^2\right)\left(\bar{q}^2 - (1-\bar{m}_c)^2\right)$$

- The fully inclusive spectrum was computed numerically with the precision of 60 significant digits for 682 points in the $(q^2/m_b^2, m_c/m_b) \equiv (\bar{q}^2, \bar{m}_c)$ space, ranging from $\bar{m}_c = 0.14$ to $\bar{m}_c = 0.33$. The triple-charm correction was computed for 650 points.
- The results were used to perform a fits with the following ansatz:

$$\frac{d\Gamma^{(2)}_{3c}}{dq^2} = m_b^3 G_F^2 |V_{cb}|^2 L_{3c}^{\frac{7}{2}} \sum_{jk} C^{(3c)}_{jk} \bar{m}_c^j \bar{q}^{2k}, \qquad L_{3c} \equiv \left(\bar{q}^2 - (1+3\bar{m}_c)^2\right)\left(\hat{q}^2 - (1-3\bar{m}_c)^2\right)$$

$$\frac{d\Gamma^{(2)}_{1c}}{dq^2} = m_b^3 G_F^2 |V_{cb}|^2 L_{1c} \sum_{jkl} C^{(1c)}_{jkl} \bar{m}_c^j \bar{q}^{2k} \log^l L_{1c}, \quad L_{1c} \equiv \left(\bar{q}^2 - (1+\bar{m}_c)^2\right)\left(\bar{q}^2 - (1-\bar{m}_c)^2\right)$$

- The results of the single-charm fit were compared with the analytic formula for $\mathcal{O}(15000)$ points. The relative error does not exceed 0.0008.

- The fully inclusive spectrum was computed numerically with the precision of 60 significant digits for 682 points in the $(q^2/m_b^2, m_c/m_b) \equiv (\bar{q}^2, \bar{m}_c)$ space, ranging from $\bar{m}_c = 0.14$ to $\bar{m}_c = 0.33$. The triple-charm correction was computed for 650 points.
- The results were used to perform a fits with the following ansatz:

$$\frac{d\Gamma^{(2)}_{3c}}{dq^2} = m_b^3 G_F^2 |V_{cb}|^2 L_{3c}^{\frac{7}{2}} \sum_{jk} C^{(3c)}_{jk} \bar{m}_c^j \bar{q}^{2k}, \qquad L_{3c} \equiv \left(\bar{q}^2 - (1+3\bar{m}_c)^2\right)\left(\hat{q}^2 - (1-3\bar{m}_c)^2\right)$$

$$\frac{d\Gamma^{(2)}_{1c}}{dq^2} = m_b^3 G_F^2 |V_{cb}|^2 L_{1c} \sum_{jkl} C^{(1c)}_{jkl} \bar{m}_c^j \bar{q}^{2k} \log^l L_{1c}, \quad L_{1c} \equiv \left(\bar{q}^2 - (1+\bar{m}_c)^2\right)\left(\bar{q}^2 - (1-\bar{m}_c)^2\right)$$

- The results of the single-charm fit were compared with the analytic formula for $\mathcal{O}(15000)$ points. The relative error does not exceed 0.0008.
- The error of the triple-charm fit is smaller than 1.4% when compared with numerical results.

- Normalized spectrum of the single-charm channel in the on-shell scheme at the NNLO.

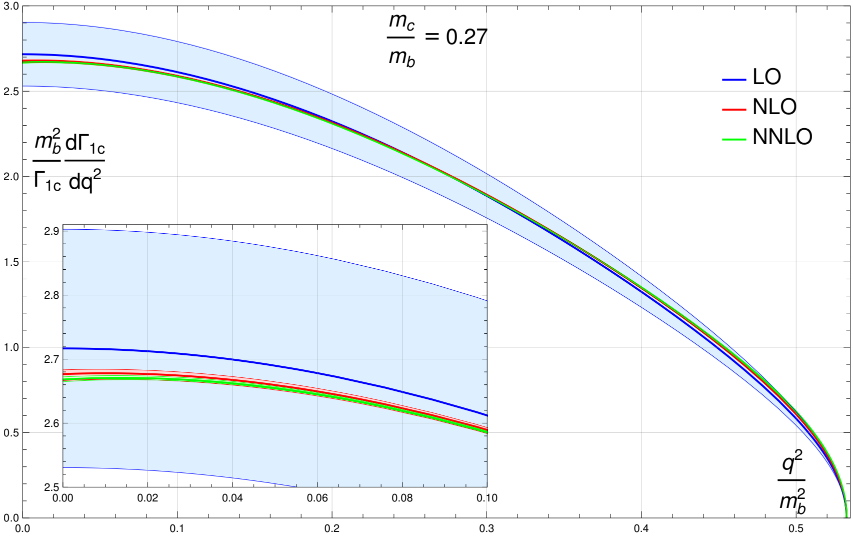

- The LO error was estimated as $\pm\alpha_s(m_b)\mathrm{LO}/\pi$.
- The NLO and NNLO errors come from varying the renormalization scale between $m_b/2$ and $2m_b$.

- The first four centralized q^2 moments in the on-shell scheme as functions of the q^2_{cut}.

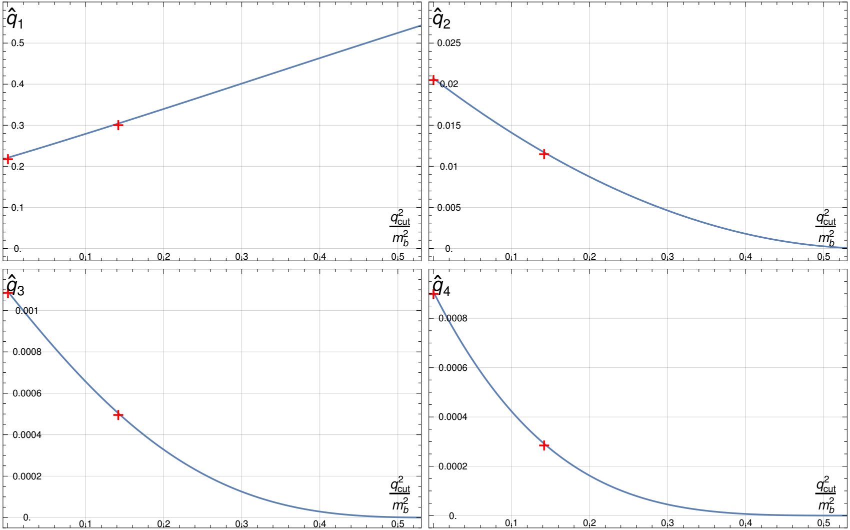

- Red crosses (+) depict results quoted from [M. Fael and F. Herren, JHEP 05 (2024) 287].

- The leading normalized spectrum of the triple-charm channel.

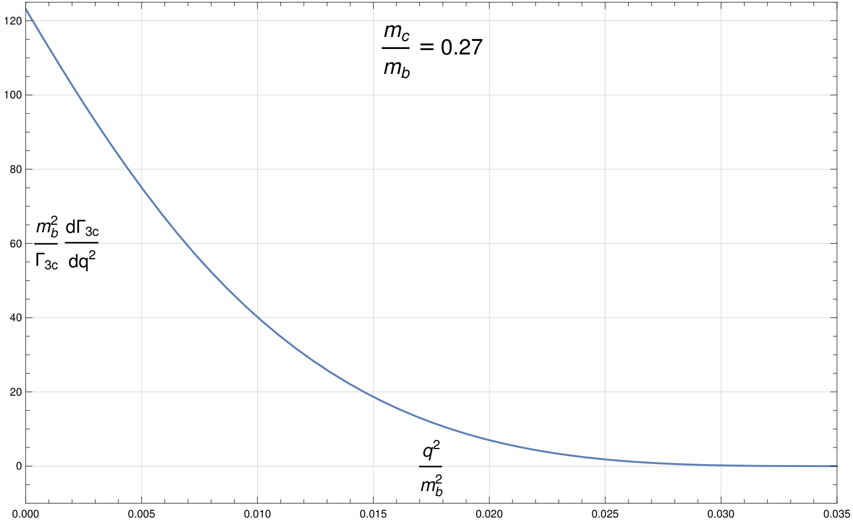

- The probability of the triple-charm decay decreases rapidly with m_c.

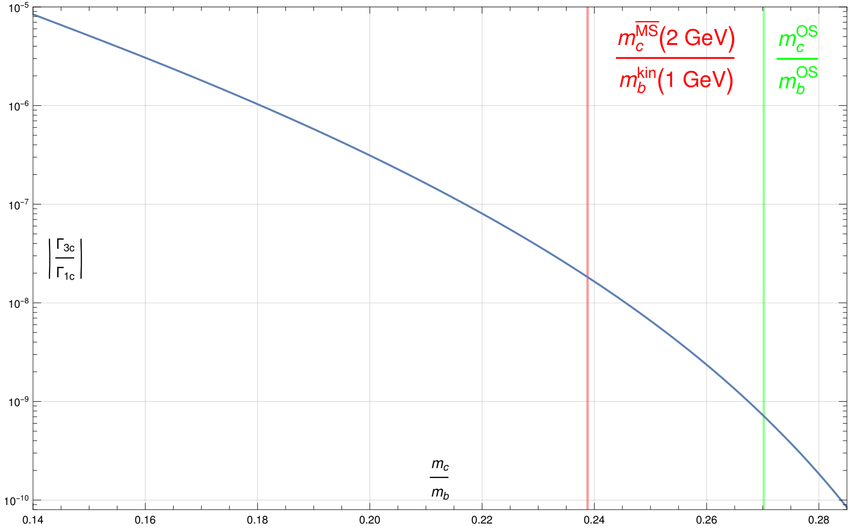

- The relative impact of the triple-charm channel on the NNLO correction to the centralized moments.

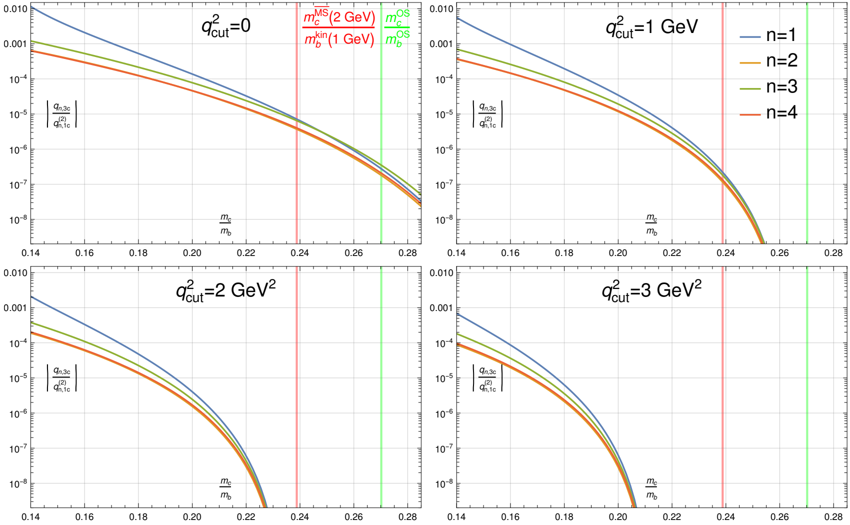

Conclusions

- The q^2 spectrum of the inclusive semileptonic decay can play an important role for semileptonic fits due to its RP invariance.
- The partonic contribution to the q^2 spectrum is now available up to $\mathcal{O}(\alpha_s^2)$.
- The analytic form of the $\mathcal{O}(\alpha_s^2)$ correction to the single-charm channel was published in [M. Fael and F. Herren, JHEP 05 (2024) 287] and independently confirmed by a dense numerical scan using the auxiliary mass flow method.
- The triple-charm q^2 spectrum was found as a fit of elementary functions to a numerical scan.
- Its contribution can impact the semileptonic fits only for very low values of q^2_{cut} and m_c/m_b.